arXiv:cond-mat/0405705v1 [cond-mat.str-el] 31 May 2004

Electron Dynamics in a Coupled Quantum Point Contact Structure with a Local Magnetic Moment *

Vadim I. Puller and Lev G. Mourokh

Department of Physics and Engineering Physics,

Stevens Institute of Technology, Hoboken, New Jersey 07030, USA

A. Shailos and J. P. Bird

Department of Electrical Engineering and Center for Solid State Electronics Research,

Arizona State University, Tempe, Arizona, 85287-5706, USA

Abstract

We develop a theoretical model for the description of electron dynamics in coupled quantum wires when the local magnetic moment is formed in one of the wires. We employ a single-particle Hamiltonian that takes account of the specific geometry of potentials defining the structure as well as electron scattering on the local magnetic moment. The equations for the wave functions in both wires are derived and the approach for their solution is discussed. We determine the transmission coefficient and conductance of the wire having the local magnetic moment and show that our description reproduces the experimentally observed features.

* Based on work presented at 2004 IEEE NTC Quantum Device Technology Workshop

I. INTRODUCTION

The low-temperature conductance of quantum point contacts (QPCs) is well known to be quantized in units of $2e^2/h$, a phenomenon that can be explained in terms of a simple transmission (Landauer) picture in which the influence of electron-electron interactions is neglected [1]. While this model is remarkably successful in accounting for the observation of conductance steps at integer units of $2e^2/h$, it is unable to explain the origin of the additional conductance plateau, observed near $0.7 \cdot 2e^2/h$ in numerous experiments. (For an overview of this issue, see Ref. [2].) While many different theoretical models have been proposed to account for the origins of the 0.7 feature, there is a wide consensus that it should be associated with some novel many-body effect. In particular, there is growing consensus that this feature is associated with the development of a net magnetic moment in the QPC [3, 4, 5]. In our recent work [6], we have explored the use of coupled quantum wires as a means for providing electrical detection of the local-moment formation. The device structure that we have studied is shown in Fig. 1 and was formed in the two-dimensional electron gas of a GaAs/AlGaAs quantum well. The device was realized by means of electron-beam lithography, and lift-off of Ti-Au gates. These gates were formed on a Hall bar with eight ohmic contacts, positioned uniformly along its upper and lower edges. In suitable combinations, these contacts could be used to make four-probe measurements of the conductance of either wire, or of the quantum dot itself (as indicated in Fig. 1). Of particular interest here is the non-local measurement (right panel) that can be made by measuring the conductance through one (fixed) wire as the gate voltage (V_g) applied to the other (swept) wire is varied. The key result of our experiment is that as the swept wire pinches off, a resonant enhancement of the conductance of the fixed wire is observed. A convincing theoretical explanation for this resonant interaction was provided in a subsequent theoretical report by our group [7]. Based on a modified Anderson Hamiltonian, we have shown that the resonant interaction with the local magnetic moment formed in the swept wire leads to an additional positive contribution to the density of states of the fixed wire and, consequently, to an enhancement of its conductance. While this analysis provides a qualitative understanding of the resonant interaction between the quantum wires, the tunnel matrix elements involved in the Anderson Hamiltonian are generally unknown and have thus far been used as fitting parameters. The influence of the specific device geometry on these matrix elements has

thus far been neglected, even though geometry-related effects are known to be important for the description of scattering in one-dimensional structures [8, 9]. To overcome these shortcomings, in the present paper we develop a more comprehensive theory for electron dynamics in the coupled-wire system and attempt to calculate the amplitude of the resonant inter-wire interaction from first principles. The basic idea of this approach will be to calculate the single-electron transmission properties in a device potential that is modified by the presence of an extra scattering term, arising from the presence of a local magnetic moment in one of the wires. The formulation of this idea is given in Section II where we derive equations describing the dynamics of electrons in the swept and fixed wires. The approach to treat these equations is given in Section III, where the expression for conductance is obtained in terms of transmission matrix elements. In the present paper we restrict ourselves to the analysis of electron dynamics in the swept wire with the examination of the fixed wire to be published elsewhere [10], and in Section IV we determine the transmission coefficient and conductance for the swept wire. In this, we obtain experimentally observed features such as additional $0.75 \cdot 2e^2/h$ plateau for the ferromagnetic coupling and $0.25 \cdot 2e^2/h$ plateau for the antiferromagnetic coupling [11, 12]. The conclusions are presented in Section V.

II. ELECTRON MODES IN THE COUPLED QUANTUM WIRE STRUCTURE

We start our description of electron dynamics in the coupled quantum wire structure from the following single-particle Hamiltonian

$$\hat{H}_0 = K_x + K_y + U(x) + W(y) + V(x,y) - J(x,y)\hat{\vec{\sigma}} \cdot \hat{\vec{S}}, \tag{1}$$

where K_x and K_y are the kinetic energy operators for the electron localized in 2D plane, $W(y)$ is the double-well potential describing the two quantum wires (Fig.2, center panel), $V(x,y)$ is the potential of the tunnelling channel connecting the two wires (Fig.2, right panel), and $U(x)$ describes the smooth bottleneck shape of the quantum wire channels. The last term simulates exchange coupling between the conductance electrons (Pauli matrices $\hat{\vec{\sigma}}$) and the local moment, $\hat{\vec{S}}$, which is assumed to be a spin-1/2 magnetic moment with $J(x,y)$ as the coordinate-dependent exchange coupling constant. The potentials $U(x), J(x,y)$, and $V(x,y) \longrightarrow 0$ as $x \longrightarrow \pm\infty$. The potential $V(x,y)$ is very sharp in comparison with the variation of $U(x)$ in the x-direction. $J(x,y)$ has an x-dependence similar

to that of $U(x)$, since the spatial characteristics of the local magnetic moment formed in the conducting channel are determined by the shape of this channel.

We write the Schrödinger equation in the form

$$\hat{H}_0\hat{\psi}(x,y) = E\hat{\psi}(x,y), \tag{2}$$

where the symbol "hat" in this and other equations is used for operators and wave functions in the four-dimensional spin space of the two spins. The basis vectors in this space are given by [13]

$$\hat{\chi}_1 = |\uparrow_e\rangle\,|\uparrow_S\rangle\,,\ \hat{\chi}_2 = |\downarrow_e\rangle\,|\downarrow_S\rangle\,,\hat{\chi}_3 = |\uparrow_e\rangle\,|\downarrow_S\rangle\,,\ \text{and}\ \hat{\chi}_4 = |\downarrow_e\rangle\,|\uparrow_S\rangle\,, \tag{3}$$

where $|\uparrow_e\rangle$ ($|\downarrow_e\rangle$) and $|\uparrow_S\rangle$ ($|\downarrow_S\rangle$) are spin-up (spin-down) states of the electron spin, $\vec{\sigma}$, and the local moment spin, $\vec{S}$, respectively.

The solution of the Schrödinger equation, Eq. (2), can be expanded in terms of the spin functions, Eq. (3), as

$$\hat{\psi}(x,y) = \sum_{\alpha=1}^{4} \chi_\alpha \psi_\alpha(x,y). \tag{4}$$

It should be noted that the Hamiltonian, Eq. (1), is not diagonal in the spin space determined by the *uncoupled* representation, Eq. (3), due to the presence of the exchange term. This term can be diagonalized by means of a unitary transformation to the *coupled* representation with transformation operator

$$\hat{X} = \begin{pmatrix} 1 & 0 & 0 & 0 \\ 0 & 1 & 0 & 0 \\ 0 & 0 & \frac{1}{\sqrt{2}} & -\frac{1}{\sqrt{2}} \\ 0 & 0 & \frac{1}{\sqrt{2}} & \frac{1}{\sqrt{2}} \end{pmatrix}. \tag{5}$$

The wave function in the coupled representation is given by

$$\hat{\psi}'(x,y) = \hat{X}^{+}\hat{\psi}(x,y) \tag{6}$$

with $\psi'_\alpha(\alpha = 1,2,3)$ describing the triplet and with ψ'_4 describing the singlet spin states. It should be emphasized that for $x \longrightarrow \pm\infty$ the Hamiltonian is diagonal in the uncoupled representation due to the vanishing of potentials $U(x) = 0$, $V(x,y)$ and $J(x,y) = 0$.

Following the procedure of Ref. [8] we expand the full wave functions in terms of different propagating modes

$$\hat{\psi}(x,y) = \sum_n \hat{\varphi}_n(x)\Phi_n(y) \tag{7}$$

with the transverse structure of n-th mode given by the solutions of the equation

$$[K_y + W(y)]\,\Phi(y) = E_n \Phi_n(y). \tag{8}$$

Correspondingly, the wave functions $\hat{\varphi}_n(x)$ obey the coupled equations

$$[E - E_n - K_x - U_n(x)]\,\hat{\varphi}_n(x) = \sum_{m \neq n} \left(V_{nm}(x) - J_{nm}(x)\hat{\vec{\sigma}} \cdot \hat{\vec{S}} \right) \hat{\varphi}_m(x) \tag{9}$$

where

$$V_{nm}(x) = \int dy \Phi_n^*(y) V(x,y) \Phi_m(y), \tag{10}$$

$$J_{nm}(x) = \int dy \Phi_n^*(y) V(x,y) \Phi_m(y), \tag{11}$$

and $U_n = U(x) + V_{nn}(x)$.

In the following analysis we make a number of simplifications in Eq. (9). First, we note that if the wires are well separated, the wave functions $\Phi_n(y)$ are strongly localized in one of the two wires, therefore we can distinguish the modes propagating in each of the wires. We assume that the shape of the confining potential $W(y)$ is such that one of the wires is close to pinch off (*swept* wire), i.e. it has only one propagating mode (described by the wave function $\hat{\varphi}_0(x)$) with the transverse confinement (subband bottom) energy, E_n, less than the Fermi energy, whereas the other wire (*fixed* wire) has several propagating modes. The localized magnetic moment is supposed to form in the only subband of the swept wire, hence the exchange coupling can be approximated as $J_{nm}(x) = \delta_{n,0}\delta_{m,0}J(x)$. Thus the system of equations is reduced to

$$\left[E - E_0 - K_x - U_0(x) + J(x)\hat{\vec{\sigma}} \cdot \hat{\vec{S}} \right] \hat{\varphi}_0(x) = \sum_{n \geq 1} V_{0n}(x) \hat{\varphi}_n(x) \tag{12}$$

and

$$[E - E_n - K_x - U_n(x)]\,\hat{\varphi}_n(x) = \sum_m V_{nm}(x) \hat{\varphi}_m(x). \tag{13}$$

Furthermore, relying on the large energy separation between the subbands in comparison with the magnitudes of $V_{nm}(x)$ and $J(x)$, we restrict our analysis to a two-subband model, keeping only the subband in the fixed wire whose energy is the closest to that of the swept

wire (the wave function of this subband is $\hat{\varphi}_1(x)$) with the resulting set of equations given by

$$\left[E - E_0 - K_x - U_0(x) + J(x)\hat{\vec{\sigma}} \cdot \hat{\vec{S}}\right] \hat{\varphi}_0(x) = V(x)\hat{\varphi}_1(x), \tag{14}$$

$$\left[E - E_1 - K_x - U_1(x)\right] \hat{\varphi}_1(x) = V(x)\hat{\varphi}_0(x), \tag{15}$$

where we have introduced $V(x) = V_{01}(x) = V_{10}(x)$.

Eqs. (14,15) can be decoupled using Green's functions:

$$\hat{G}_0(\epsilon) = \left[\epsilon - K_x - U_0(x) + J(x)\hat{\vec{\sigma}} \cdot \hat{\vec{S}}\right]^{-1} \tag{16}$$

and

$$\hat{G}_1(\epsilon) = \left[\epsilon - K_x - U_1(x)\right]^{-1}. \tag{17}$$

With these Green's functions Eqs. (14,15) can be formally integrated as

$$\hat{\varphi}_0(x) = \hat{G}_0(E - E_0)V(x)\hat{\varphi}_1(x) \tag{18}$$

and

$$\hat{\varphi}_1(x) = \hat{G}_1(E - E_1)V(x)\hat{\varphi}_0(x). \tag{19}$$

Accordingly, we obtain

$$\left[E - E_0 - K_x - U_0(x) + J(x)\hat{\vec{\sigma}} \cdot \hat{\vec{S}}\right] \hat{\varphi}_0(x) = V(x)\hat{G}_1(E - E_1)V(x)\hat{\varphi}_0(x), \tag{20}$$

and

$$\left[E - E_1 - K_x - U_1(x)\right] \hat{\varphi}_1(x) = V(x)\hat{G}_0(E - E_0)V(x)\hat{\varphi}_1(x). \tag{21}$$

The Green's function $\hat{G}_1(\epsilon)$ is a scalar Green's function, i.e. it is a unit matrix in the uncoupled spin space, whereas $\hat{G}_0(\epsilon)$ has a more complicated structure. Nevertheless, it can be expressed in terms of two scalar Green's functions [10] as

$$\hat{G}_0(\epsilon) = \frac{1}{4}\left[3g^t(\epsilon) + g^s(\epsilon)\right]\hat{I} + \frac{1}{4}\left[g^t(\epsilon) - g^s(\epsilon)\right]\hat{\vec{\sigma}} \cdot \hat{\vec{S}}, \tag{22}$$

where

$$g^t(\epsilon) = \left[\epsilon - K_x - U(x) + J(x)\right]^{-1} \tag{23}$$

and

$$g^s(\epsilon) = \left[\epsilon - K_x - U(x) - 3J(x)\right]^{-1}. \tag{24}$$

Now we are able to redefine the scalar potentials, as

$$\tilde{U}_0(x,E) = U_0(x) + V(x)\hat{G}_1(E-E_1)V(x) \tag{25}$$

and

$$\tilde{U}_1(x,E) = U_1(x) + V(x)\frac{1}{4}\left[3g^t(E-E_0) + g^s(E-E_0)\right]V(x), \tag{26}$$

and introduce the tunneling-induced exchange coupling of electrons in the fixed wire to the local magnetic moment,

$$j(x,E) = -V(x)\frac{1}{4}\left[g^t(E-E_0) - g^s(E-E_0)\right]V(x). \tag{27}$$

As a result, we obtain equations for the description of electron dynamics in the swept and fixed wires in the form

$$\left[E - E_0 - K_x - \tilde{U}_0(x) + J(x)\hat{\vec{\sigma}}\cdot\hat{\vec{S}}\right]\hat{\varphi}_0(x) = 0, \tag{28}$$

and

$$\left[E - E_1 - K_x - \tilde{U}_1(x) + j(x)\hat{\vec{\sigma}}\cdot\hat{\vec{S}}\right]\hat{\varphi}_1(x) = 0. \tag{29}$$

Although the form of these two equations is very similar, and they can be both treated in the same manner (as is discussed in the next Section), the results they yield will differ, depending on the specific shapes of the potentials and exchange couplings. In particular, while the shape of the coupling $J(x)$ in Eq. (28) is smooth, similar to that of the potential $U(x)$, the exchange constant $j(x)$ of Eq. (29) is proportional to the potential $V(x)$, and therefore is sharper than the bottleneck potential $U(x)$.

III. ELECTRON SCATTERING BY A LOCALIZED SPIN

In this Section we determine the transmission coefficient and, correspondingly, the conductance of the quantum wire channel in the presence of electron scattering from a magnetic moment. The equation for the electron wave function in the uncoupled representation has the form [13]

$$\left(\epsilon - K_x - U(x) + J(x)\vec{\sigma}\cdot\vec{S}\right)\hat{\varphi}(x) = 0. \tag{30}$$

We are looking for a scattering solution of this equation with incident wave of the form $\hat{A}e^{ikx}$, i.e. for a wave incident from $x=-\infty$ and having momentum $\hbar k = \sqrt{2m\epsilon}$. Here, $\hat{A}$

is also the vector in the spin space,

$$\hat{A} = \sum_{\alpha=1}^{4} A_\alpha \hat{\chi}_\alpha, \tag{31}$$

with $w_\alpha = |A_\alpha|^2$ being the probability to have the certain initial orientation for the electron and magnetic moment spins.

In the present paper we generalize the approach of Ref. [13] (where the coupling constant $J(x)$ was assumed to be a δ-function) to the case of a real spatial dependence of the coupling constant. To accomplish this, we find a solution of Eq. (30) for the wave function in the coupled representation and find the transmission coefficient for the wave function in the uncoupled representation by means of unitary transformation of Eq. (5). For the triplet and singlet states of the coupled representation, Eq. (30) has the form

$$\left(\epsilon - K_x - U(x) + J(x)\right) \phi_k^{t\pm}(x) = 0 \tag{32}$$

and

$$\left(\epsilon - K_x - U(x) - 3J(x)\right) \phi_k^{s\pm}(x) = 0, \tag{33}$$

where indices t and s denote the triplet and singlet solutions, respectively. The scattering solutions of these equations have the following asymptotic behavior [8]

$$\phi_k^{t,s+}(x) = \begin{cases} T_{t,s} e^{ikx}, & x \longrightarrow +\infty \\ e^{ikx} + R_{t,s+} e^{-ikx}, & x \longrightarrow -\infty \end{cases} \tag{34}$$

and

$$\phi_k^{t,s-}(x) = \begin{cases} e^{-ikx} + R_{t,s-} e^{ikx}, & x \longrightarrow +\infty \\ T_{t,s} e^{ikx}, & x \longrightarrow -\infty \end{cases}, \tag{35}$$

and the transmission coefficient of the wave functions in the uncoupled representation can be obtained [10] as

$$\hat{T} = \begin{pmatrix} T_t & 0 & 0 & 0 \\ 0 & T_t & 0 & 0 \\ 0 & 0 & \frac{1}{2}\left(T_t + T_s\right) & \frac{1}{2}\left(T_t - T_s\right) \\ 0 & 0 & \frac{1}{2}\left(T_t - T_s\right) & \frac{1}{2}\left(T_t + T_s\right) \end{pmatrix} \tag{36}$$

Now we can use the Landauer-Büttiker formula [14, 15] to determine the conductance of the quantum wire:

$$G = \frac{2e^2}{h} \sum_{\alpha,\beta} |T_{\alpha\beta}|\, w_\beta \tag{37}$$

where w_β gives the probability of initial spin configuration. With the transmission matrix given by Eq. (36), the conductance becomes

$$G = \frac{2e^2}{h}\left[|T_t|^2\,(w_1+w_2) + \frac{1}{2}\left(|T_t|^2 + |T_s|^2\right)(w_3+w_4)\right] \tag{38}$$

and, with account for the normalization of probability, $\sum_{\alpha=1}^{4} w_\alpha = 1$, it takes the form

$$G = \frac{2e^2}{h}\left[|T_t|^2 + \frac{1}{2}\left(|T_s|^2 - |T_t|^2\right)(w_3+w_4)\right]. \tag{39}$$

IV. CONDUCTANCE OF THE SWEPT WIRE

In this section we show how our model for the local magnetic moment reproduces the correct conductance behavior when the swept wire is pinched off. As the basis for our analysis we use the expression for the conductance, Eq. (39), jointly with our assumption that the potential $U_0(x)$ and the exchange coupling $J(x)$ are smooth functions in comparison to the electron wavelength, $\lambda = 2\pi/k$. It should be noticed that the potential $\tilde{U}_0(x)$ in Eq. (28) is not very smooth due to the additional contribution of a sharp potential $V(x)$ (see Eq. (23)), however our analysis is still valid as long as this additional contribution is small in comparison to $J(x)$.

Functions $\tilde{U}_0(x)$ and $J(x)$ can be expanded into series near their maxima. Since the two functions are smooth we can assume that they take their maximum values at the same point $x = 0$. These expansions are given by

$$\tilde{U}_0(x) = \tilde{U}_0(0) + \frac{x^2}{2}\frac{\partial^2 \tilde{U}_0(x)}{\partial x^2}|_{x=0} = U_{max} - \frac{m\omega_U^2 x^2}{2} \tag{40}$$

and

$$J(x) = J(0) + \frac{x^2}{2}\frac{\partial^2 J(x)}{\partial x^2}|_{x=0} = J_{max} - \frac{m\omega_J^2 x^2}{2}. \tag{41}$$

Equations (32,33), defining the transmission coefficients T_t and T_s, contain the effective potentials $U_+(x) = \tilde{U}_0(x) - J(x)$ and $U_-(x) = \tilde{U}_0(x) + 3J(x)$. In view of Eqs. (40,41), these potentials can be treated as inverse parabolic near their top, as

$$U_+(x) = U_{max} - J_{max} - \frac{m\omega_-^2 x^2}{2} \tag{42}$$

and

$$U_-(x) = U_{max} + 3J_{max} - \frac{m\omega_+^2 x^2}{2}, \tag{43}$$

where $\omega_- = \sqrt{\omega_U^2 - \omega_J^2}$, $\omega_+ = \sqrt{\omega_U^2 + 3\omega_J^2}$.

The transmission coefficient for the inverse parabolic barrier $u(x) = -m\omega^2 x^2/2$ is given by [16]

$$t(\eta) = \left[1 + e^{-2\pi\eta}\right]^{-1/2}, \tag{44}$$

where $\eta = \epsilon/\hbar\omega$, and the energy, ϵ, is measured from the top of the barrier. Thus, for our situation we obtain

$$T_t = t\left(\frac{\epsilon - U_{max} + J_{max}}{\hbar\omega_-}\right) \tag{45}$$

and

$$T_s = t\left(\frac{\epsilon - U_{max} - 3J_{max}}{\hbar\omega_+}\right). \tag{46}$$

The most important feature of these transmission coefficients is that the transmission probability, $|t(\eta)|^2$, is very close to the step function.

Now we are able to calculate the conductance using Eq. (39). We assume the equivalence of all initial spin orientations, i.e. $w_\alpha = 1/4$, and the conductance through the swept wire takes the form

$$G = \frac{2e^2}{h}\left[\frac{3}{4}\left|t\left(\frac{\epsilon - U_{max} + J_{max}}{\hbar\omega_-}\right)\right|^2 + \frac{1}{4}\left|t\left(\frac{\epsilon - U_{max} - 3J_{max}}{\hbar\omega_+}\right)\right|^2\right]. \tag{47}$$

The step-like structure of the transmission probability causes the conductance to reproduce the step-like behavior of 0.7-anomaly. In case of ferromagnetic coupling between the electrons and local magnetic moment, $J_{max} > 0$ our model gives an additional conductance step at $0.75 \times 2e^2/h$, as

$$G = \frac{2e^2}{h}\begin{cases} 0, & \text{if } \epsilon < U_{max} - J_{max}, \\ 0.75, & \text{if } U_{max} - J_{max} < \epsilon < U_{max} + 3J_{max}, \\ 1, & \text{if } \epsilon > U_{max} + 3J_{max}. \end{cases} \tag{48}$$

It is interesting to point out that for antiferromagnetic coupling , $J_{max} < 0$, we obtain the a conductance step at $0.25 \times 2e^2/h$, which has been observed in experiments [10] and density-functional simulations [4], as

$$G = \frac{2e^2}{h}\begin{cases} 0, & \text{if } \epsilon < U_{max} - 3\left|J_{max}\right|, \\ 0.25, & \text{if } U_{max} - 3\left|J_{max}\right| < \epsilon < U_{max} + \left|J_{max}\right|, \\ 1, & \text{if } \epsilon > U_{max} + \left|J_{max}\right|. \end{cases} \tag{49}$$

V. CONCLUSION

In conclusion, we have examined electron dynamics in coupled quantum wires under conditions where a local magnetic moment is formed in one of the wires. In our theoretical model, the single-particle Hamiltonian has been employed with account of the specific geometry defining the structure as well as electron scattering on the local magnetic moment. We have derived the coupled set of equations for the wave functions of electrons in both wires and have been able to decouple them obtaining equations describing electron dynamics in each of the two wires. While our analysis of electron processes in the fixed wire will be published elsewhere [10], we determine the transmission coefficient and conductance of the swept wire (having the local magnetic moment) and show that our description reproduces the experimentally observed features such as additional plateaus in the conductance at $0.75 \cdot 2e^2/h$ (for the ferromagnetic coupling between electrons and the local magnetic moment) and at $0.25 \cdot 2e^2/h$ (in the case of the antiferromagnetic coupling).

---

[1] S. Datta, *Electron Transport in Mesoscopic Systems*, Cambridge University Press, UK (1995).

[2] J. P. Bird and Y. Ochiai, Science **303**, 1621 (2004).

[3] Y. Meir, K. Hirose, and N. S. Wingreen, Phys. Rev. Lett. **89**, 196802 (2002).

[4] K.-F. Berggren and I. I. Yakimenko, Phys. Rev. B **66**, 085323 (2002).

[5] K. Hirose, Y. Meir, and N. S. Wingreen, Phys. Rev. Lett. **90**, 026804 (2003).

[6] T. Morimoto, Y. Iwase, N. Aoki, T. Sasaki, Y. Ochiai, A. Shailos, J. P. Bird, M. P. Lilly, J. L. Reno, and J. A. Simmons, Appl. Phys. Lett. **82**, 3952 (2003).

[7] V. I. Puller, L. G. Mourokh, A. Shailos, and J. P. Bird, Phys. Rev. Lett. **92**, 96802 (2004).

[8] S. A. Gurvitz and Y. B. Levinson, Phys. Rev. B **47**, 10578 (1993).

[9] J. U. Nöckel and A. D. Stone, Phys. Rev. B **50**, 17415 (1994).

[10] V. I. Puller, L. G. Mourokh, A. Shailos, and J. P. Bird, to be published.

[11] T. Rejec, A. Ramšak, and J. H. Jefferson, Phys. Rev. B **62**, 12985 (2000).

[12] V. V. Flambaum and M. Yu. Kuchiev, Phys. Rev. B **61**, R7869 (2000).

[13] Ch. Kunze and Ph. Bagwell, Phys. Rev. B **51**, 13410 (1995).

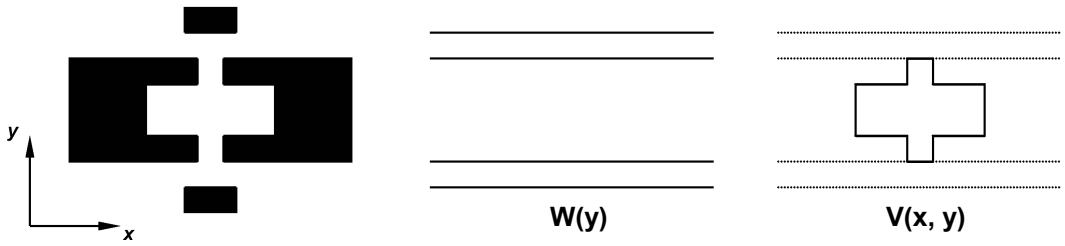
[14] R. Landauer, IBM J. Res. Dev. **1**, 223 (1957).

[15] M. Büttiker, Y. Imry, R. Landauer, and S. Pinhas, Phys. Rev. B **31**, 6207 (1985).

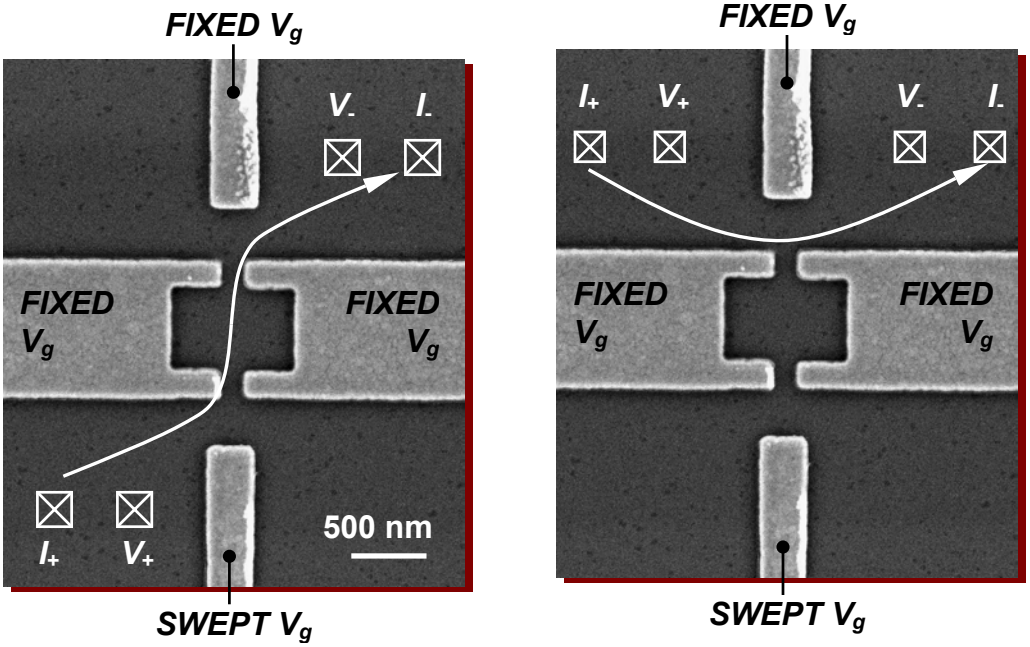
[16] see e.g., Y. B. Levinson, M. I. Lubin, and E. V. Sukhorukov, Phys. Rev. B **45**, 11936 (1992).

FIG. 1: Electron micrographs of the critical region of the device, indicating the two measurement configurations

FIG. 2: The figure on the left is a schematic of the experimental structure. The confining potential associated with this structure is modeled as a sum of potentials defining the two wires, $W(y)$, (center) and defining the tunnel channel between them, $V(x, y)$, (right).



Puller, et al., Figure 2 of 2.



Puller, et al., Figure 1 of 2.